

# The Signs of Quantum Dot-Lead Matrix Elements: The Effect on Transport vs. Spectral Properties

Alessandro Silva, Yuval Oreg\* and Yuval Gefen.

*Dept. of Condensed Matter Physics, The Weizmann Institute of Science, 76100 Rehovot, Israel.*

A small quantum dot coupled to two external leads is considered. Different signs of the dot-leads coupling matrix elements give rise to qualitatively different behavior of physical observables such as the conductance, the phase of the transmission amplitude and the differential capacitance of the dot. For certain relative signs the conductance may vanish at values of the gate potential, where the spectral density is maximal. Zeroes of the conductance are robust against increasing the dot-lead coupling. They are associated with abrupt phase lapses in the transmission phase whose width vanishes as the square of the temperature. We carefully distinguish between phase lapses of  $-\pi$  and phase anti-lapses of  $\pi$ .

PACS number(s): 73.23.Ad, 73.23.Hk, 03.65.Xp.

## I. INTRODUCTION

Two interesting directions in the study of quantum dots (QDs) have emerged in recent years. First, it has become clear that as the dot-lead coupling is increased, the effect of the Coulomb Blockade is greatly suppressed, yet does not altogether disappear. Works discussing the physics of strongly coupled QDs include Refs. 1–3 (see also Ref. 4). Second, experiments addressing the *phase* of the electron transmitted through a QD [employing an Aharonov-Bohm (AB) set-up] revealed interesting and often intriguing physics<sup>5</sup>.

Of the large number of theoretical works that followed, a few have addressed (either explicitly or implicitly) the role of the signs of the dot-lead coupling matrix elements<sup>6,7</sup>. No systematic study of the effect of the magnitude and the relative sign of these coupling matrix elements on a number of physical quantities, such as linear conductance, the spectral density and the transmission phase has been carried out to date.

A small QD (or a small electron droplet), where the electron spectrum is discrete, is a possible nanoscale laboratory for the study of interference. [The discreteness of the spectrum of a small dot is relevant when the mean level spacing  $\Delta \gg \Gamma, k_B T$ , where  $\Gamma$  is the characteristic strength of the coupling to the leads (cf. Eq.(8) below) and  $T$  is the temperature.] Indeed, in such systems there are various paths which interfere and contribute to the conductance. These correspond to different ways to traverse the QD, taking advantage of the various single particle levels. An efficient way to probe the effect of such interference on the transmission amplitude through the QD (magnitude and phase) is to embed the QD in one arm of an AB interferometer.

In a typical experimental set up the QD is connected to source and drain leads via tunneling barriers (or diffusive contacts) with a typical coupling strength  $\Gamma$ , controlled through additional gates. A “plunger gate” coupled electrostatically to the QD controls the number of electrons

in the latter<sup>8</sup>. As the potential  $V_g$  of the plunger gate is increased, electrons are pulled into the dot. When the coupling to the leads  $\Gamma$  is small ( $\Gamma \ll \Delta$ ) distinct peaks in the source-drain linear conductance occur at near-degeneracy points<sup>8</sup>, *i.e.*, when the energy of the dot with  $N$  electrons is equal to the energy of the dot with  $N + 1$  electrons (the Coulomb peaks). The peaks in conductance nearly coincide with the maxima of the derivative of the mean number of electrons in the QD with respect to  $V_g$ . The separation between the Coulomb peaks is mainly dictated by the average charging energy of the dot,  $U$ .

The main goal of the present study is to investigate the effect of the signs of the dot-lead coupling matrix elements. The underlying physics is related to the interference among different transmission amplitudes (say, from the left lead to the right lead), describing different traversal paths through different single particle levels. We analyze how this affects various physical quantities, such as the linear conductance through the QD, the phase of the transmission amplitude as measured by an AB interference experiment, the spectral density of the QD, and the differential capacitance.

Reporting here the first part of our project, and attempting to simplify the problem (ignoring some of the complex but interesting ingredients), we consider spinless electrons and ignore at this point electron-electron interactions. We also model the spectrum of the small dot by two single particle levels. In a subsequent work we will address the issue of an interacting QD. Below (see Sect. VI) we briefly comment on the relevance of studying such a toy model for the sake of gaining insight into the physics of “real life” QD.

We find that in addition to the strength of the coupling,  $\Gamma$ , the key to understand the physics of the relevant physical observables is the *relative phase* of the coupling matrix elements of consecutive orbital levels in the QD to the leads. This will be defined more accurately below. Also, we find that the dependence of the conductance and the differential capacitance (or the spectral density) as a

function of  $V_g$  are complementary. For example, when the two consecutive levels are *in phase* (*i.e.*, the signs of the respective couplings of level 1 and level 2 are identical), the conductance exhibits two peaks whose positions are unaffected by  $\Gamma$ . By contrast, the two peaks of the spectral density (hence the differential capacitance) approach each other as  $\Gamma$  is increased, eventually merging into a single peak. The complementarity is summarized in Table. I below.

It should be noted that the mean number of electrons on the dot depends only on the energy spectrum of the dot and the level width (given by diagonal matrix elements of the single electron propagator). By contrast, the conductance depends also on the actual value of the eigenfunction of the system (including off-diagonal matrix elements of the single electron propagator<sup>9</sup>). Hence it is not surprising that over a certain range of values of  $\Gamma$  the conductance and the differential capacitance exhibit qualitatively different behavior<sup>12</sup> as a function of  $V_g$ .

Another quantity which receives much attention here is the phase of the total transmission amplitude. When the signs of the respective couplings of the two dot's levels are identical (the *in-phase* scenario), it turns out that there is a value of  $V_g$  (corresponding to the “conductance valley” between the two conductance peaks) for which the zero temperature conductance vanishes. This vanishing of the conductance is associated with a lapse of the transmission phase. It turns out (by carefully including the off-diagonal Green's functions into the calculation of the transmission amplitude, see Appendix. B) that the width of the phase lapse vanishes (like the square of the temperature). We point out in our analysis how it is possible to distinguish a  $-\pi$  phase lapse from a  $+\pi$  one, an observation which, we believe, has a greater range of validity than the specific problem considered here. Surprisingly, the width of the phase lapse is determined by the temperature, to be contrasted with the width of the conductance peak (the latter is determined by  $\text{Max}[\Gamma, T]$ ).

The remainder of the paper is organized as follows: in Sect. II we discuss the relation between measurable quantities characterizing a QD, such as the conductance, the AB oscillatory part of the conductance, the mean number of electrons, the transmission amplitude, its phase and the spectral density of electrons. In Sect. III we introduce a toy model consisting of a two level QD attached to two leads. We recall an expression for the transmission amplitude through the QD as well as for the spectral density (derivation of the latter can be found in Appendix. A). In Sect. IV we study the *in-phase* case (all four coupling matrix elements having the same sign). In Sect. V we consider the *out-of-phase* case, where one of the matrix elements has a sign opposite to the others.

Section VI includes some remarks concerning the relevance of the present analysis to the interacting case and the possible extension of our model to more than two levels.

## II. MEASURABLE QUANTITIES

Experimentally, the basic quantities characterizing transport through a QD are the conductance, the AB oscillations pattern when the QD is inserted in an AB interferometer and the differential capacitance, describing how the number of electrons occupying the QD varies as function of  $V_g$ .

Since we consider here a model of independent electrons, it is possible to relate all these quantities<sup>9,11</sup> to the transmission amplitude  $t(\omega)$  through the QD and the spectral density  $A(\omega)$ . We assume throughout our analysis single-channel transport through each participating lead.

### A. The Conductance $G$

Information about the absolute value of  $t(\omega)$  close to the Fermi level can be obtained through the linear response conductance, given by

$$G = -\frac{e^2}{h} \int d\omega f'(\omega) |t(\omega)|^2, \quad (1)$$

where  $f(\omega)$  is the Fermi function.

### B. Phase of the transmission amplitude $\theta$

It is also possible to measure the phase of the transmission amplitude through the QD by inserting it in one arm of an open geometry AB interferometer, shown schematically in Fig. 1.

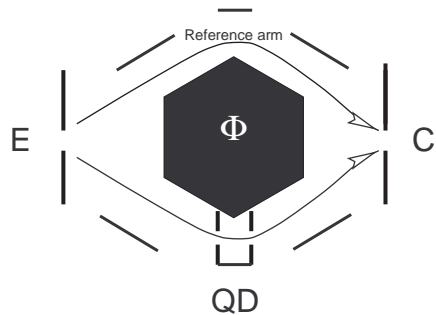


FIG. 1. Schematic picture of an open geometry AB interferometer. Electrons traverse the interferometer from the emitter (E) to the collector (C). In one of the two arms a QD is inserted; a magnetic flux  $\Phi$  is enclosed in the area of the interferometer. The two arrowed paths are those that contribute the most to the conductance in the open geometry configuration.

One measures the dependence of the linear conductance through the interferometer upon the enclosed flux,  $\Phi$ , and on the plunger gate voltage  $V_g$ . It is possible to show<sup>7,10,11</sup> that in this double-slit geometry the flux-dependent oscillatory component of the conductance is given by

$$G_{AB} \propto 2 \operatorname{Re} \left[ t_{\text{ref}}^* \left( \int d\omega (-f'(\omega)) t(\omega) \right) e^{2\pi i \Phi / \Phi_0} \right], \quad (2)$$

where  $t_{\text{ref}}$  is the transmission amplitude through the reference arm, assumed to be  $V_g$  independent ( $t_{\text{ref}}$  is taken energy independent as well);  $\Phi_0 = hc/e$  is the flux quantum. It is thus possible to extract information about the temperature weighted phase of the transmission amplitude through the QD

$$\theta(T) = \arg \left[ - \int d\omega f'(\omega) t(\omega) \right]. \quad (3)$$

In practice this is done by recording the AB oscillations as a function of  $\Phi$  for several values of the parameter  $V_g$ . The phase evolution (as a function of  $V_g$ ) can be extracted<sup>5</sup> from the relative phase shift of the various curves.

We note that the “transmission phase” so measured may not reflect the actual transmission phase through the QD, but might be affected by multiple reflection paths, reflection from any of the terminals of the interferometer and deviations from unitarity<sup>13,14</sup>.

### C. Differential Capacitance Measurements.

The spectral density  $A(\omega)$  represents the local density of states in the QD at energy  $\omega$  and is formally proportional to the imaginary part of the trace of the dot retarded Green’s function matrix (see Eq. A4). One can relate the spectral density to the average number of electrons occupying the QD through the expression

$$N = \int_{-\infty}^{\infty} \frac{d\omega}{2\pi} f(\omega) A(\omega), \quad (4)$$

and study how  $N$  varies as a function of  $V_g$ . In this case the measured quantity is the differential capacitance

$$C(V_g) = \frac{d e N}{d V_g} = e \int_{-\infty}^{\infty} \frac{d\omega}{2\pi} f(\omega) \frac{d A(\omega)}{d V_g}, \quad (5)$$

where  $e$  is the electronic charge. The differential capacitance can be measured by means of a detector sensitive to the QD charge<sup>18,19</sup>.

### III. A TOY MODEL HAMILTONIAN

We shall consider the Hamiltonian

$$H = \sum_{k,\alpha} \epsilon_{k,\alpha} c_{k,\alpha}^\dagger c_{k,\alpha} + \sum_j \epsilon_j d_j^\dagger d_j + \sum_{k,\alpha,j} \left[ V_{\alpha,j} c_{k,\alpha}^\dagger d_j + h.c. \right], \quad (6)$$

where the operators  $c_{k,\alpha}$  refer to electronic states in the leads ( $\alpha = L, R$ ) and the operators  $d_j$  describe the quantum dot levels ( $j = 1, 2$ ). In order to simplify our discussion, we will assume the dot-lead couplings  $V_{\alpha,j}$  to all have the same magnitude but possibly different phases. It is straightforward to see that three of these phases can be gauged out<sup>21</sup>, absorbing them in the definitions of the operators  $c_{k,\alpha}$  and  $d_j$ . Hence, we choose<sup>22</sup>  $V_{L,1} = V_{R,1} = V_{L,2} = V$  and  $V_{R,2} = e^{i\varphi} V$ . When time reversal symmetry is present, the QD’s wave functions can be chosen real, whereby, upon an appropriate gauge of the lead wave functions, the value of the relative phase  $\varphi$  is either 0 or  $\pi$ , in other words  $s \equiv e^{i\varphi} = \pm 1$ .

We are interested in calculating the transport properties of this model as a function of a plunger gate voltage. This can be done setting  $\epsilon_{1,2} = -\epsilon \pm \Delta/2$ , where  $\Delta = \epsilon_1 - \epsilon_2$ , and studying the behavior of the system as a function of

$$\epsilon(V_g) = \epsilon(V_g = 0) + V_g. \quad (7)$$

Other than the level spacing, the scale coming into play is the strength of the coupling to the leads

$$\Gamma = 2\pi\rho V^2, \quad (8)$$

where  $\rho$  is the density of states (DOS) of the leads.

Since the Hamiltonian is free (quadratic), the calculation of both  $t(\omega)$  and  $A(\omega)$  is straightforward (see Appendix A). One readily obtains

$$t_{\pm}(\omega) = \frac{\Gamma}{D_{\pm}(\omega)} [(\omega - \epsilon_1) \pm (\omega - \epsilon_2)], \quad (9)$$

$$A_{\pm}(\omega) = \frac{2\Gamma}{|D_{\pm}(\omega)|^2} [2\omega^2 - 2\omega(\epsilon_1 + \epsilon_2) + \epsilon_1^2 + \epsilon_2^2 + \Gamma^2(1 \mp 1)], \quad (10)$$

where the denominator  $D_{\pm}(\omega) \equiv (\omega - \epsilon_1)(\omega - \epsilon_2) + i\Gamma(2\omega - \epsilon_1 - \epsilon_2) - \Gamma^2(1 \mp 1)/2$ .

### IV. THE IN-PHASE ( $s = +1$ ) CASE

As first step in our analysis we consider the *in-phase* case,  $s = +1$  [upper sign in Eqs. (9), (10)]. Starting with the zero temperature limit, all transport properties are determined by the value of  $t(\omega)$  at the Fermi level, *i.e.*, at  $\omega = \epsilon_F \equiv 0$ . From Eq. (9) the transmission amplitude at the Fermi level can be written as

$$t_{s=+}(0) \equiv t_+ = \frac{2\Gamma\epsilon}{\epsilon^2 - (\Delta/2)^2 + 2i\Gamma\epsilon}. \quad (11)$$

We now discuss the implications to the conductance and its flux sensitive component.

### A. The conductance $G$ and the transmission-phase $\theta$ for $s = +1$

At zero temperature the Fermi function in Eq. (1) can be substituted by a Dirac delta function and  $G$  is given by  $G = (e^2/h)t_+$ . The conductance  $G$  is depicted in Fig. 2 for various values of the parameters.

The main feature to be noticed in Fig. 2 is the presence of an exact zero of the transmission probability between the two peaks, resulting from the vanishing of the numerator in Eq. (11) at  $\epsilon = 0$ . Physically that zero can be interpreted as the result of destructive interference between paths (left to right) traversing levels 1 and 2 of the dot respectively (see Appendix. B). As we demonstrate below, the interference pattern is sensitive to the relative sign  $s$ .

The existence of a zero in the transmission amplitude implies the existence of an abrupt (without a scale) phase lapse<sup>5,7,15-17</sup> of  $-\pi$  in the “conductance valley” between the two conductance peaks (cf. Fig. 3).

In terms of the AB oscillations pattern (*e.g.*, the conductance measured as a function of  $\Phi$ ) this implies that as  $\epsilon$  varies from  $0^-$  to  $0^+$   $G(\Phi)$  shifts abruptly by half a period. Since at  $T = 0$  this shift is abrupt, it is physically impossible to discuss its direction, *i.e.*, whether the phase of the AB oscillations jumps by  $-\pi$  (lapse) or by  $+\pi$  (anti-lapse). Interestingly, at finite temperatures this ambiguity is resolved: the phase varies by  $-\pi$  close to  $\epsilon = 0$  (a lapse).

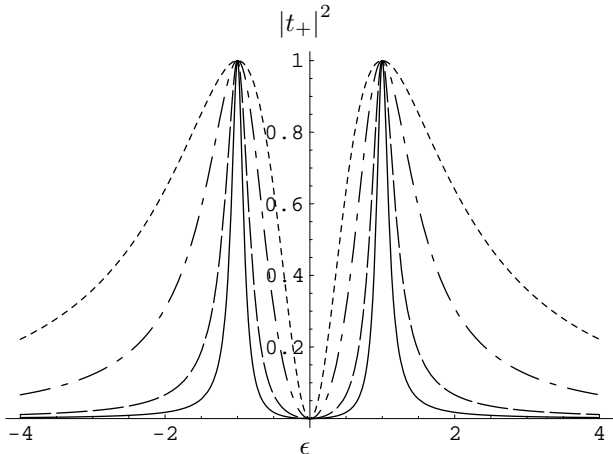


FIG. 2. Transmission probability  $|t_+|^2$  at the Fermi energy of the leads vs.  $\epsilon$  for  $s = +$ . Here  $\epsilon_1 - \epsilon_2 = 2$  and  $\Gamma = 0.1$  (full), 0.2 (dashed), 0.5 (dash-dotted), 1 (dotted). Notice that (i) at  $\epsilon = 0$  the contributions to the transmission through the two levels (including off-diagonal elements of the transmission matrix) add up destructively leading to an exact zero of the transmission probability (see Appendix. B); and (ii) the peak positions and maximal values (equal to 1) are insensitive to  $\Gamma$ . The spectral density of the  $s = -1$  case ( $A_-$  in Fig. 8) exhibits a feature similar to the latter for large values of  $\Gamma$ , while the spectral density  $A_+$  (see Fig. 5) has a maximum at  $\epsilon = 0$ .

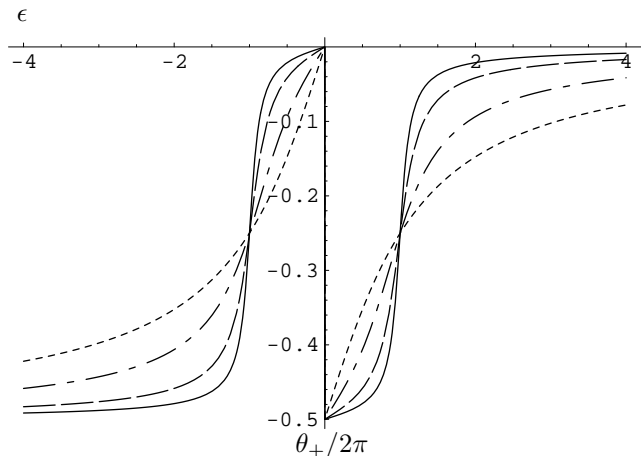


FIG. 3. The transmission phase  $\theta_+/2\pi$  at zero temperature vs.  $\epsilon$  for  $s = +$ . Here,  $\epsilon_1 - \epsilon_2 = 2$  and  $\Gamma = 0.1$  (full), 0.2 (dashed), 0.5 (dash-dotted) and 1 (dotted). Note that the destructive interference of the transmission through the dot’s levels leads to the vanishing of the conductance at  $\epsilon = 0$  which, in turn, leads to an abrupt (without a scale) phase-lapse in the “conductance valley”. As discussed below [cf. Eq. (13)], the width of the phase lapse at finite temperatures is  $\propto \Gamma T^2/\Delta^2$ , introducing a new nontrivial energy scale.

This conclusion can be obtained by noting that the trajectory in the complex plane of  $t_+$  [as a function of  $\epsilon(V_g)$ ] is a closed curve tangential to the the abscissa at the origin (cf. the black line in Fig. 4), *i.e.*,  $\text{Im}[t(\omega)] \leq 0$ . As  $\epsilon$  is swept from  $-\infty$  to  $+\infty$ , the transmission amplitude performs two full *counterclockwise* revolutions, starting from  $t(-\infty) = [0^-, 0^-]$  and ending at  $t(\infty) = [0^+, 0^-]$ . In the lower plot of Fig. 4 we show how  $t_+(\epsilon)$  makes almost two full revolutions around the circle when  $-4 < \epsilon < 4$ . It starts (for  $\epsilon = -4$ ) at  $[\text{Re}(t_+), \text{Im}(t_+)] \approx [-0.3, -0.05]$ , goes through point (a) (cf. the upper plot of Fig. 4) then proceeds to point (b) at the origin and goes around the circle through point (c).

For a fixed  $\epsilon$  at finite temperatures, one needs to average over the sections of the curve close to  $t_+(\epsilon)$ , with the appropriate statistical weight [cf. Eq. (C2)]. The result is a trajectory (shown schematically as a grey contour in Fig. 4) which does not include the origin; the phase  $\theta_+(T)$  evolves from  $-\pi$  to 0 with a lapse of a finite width at  $\epsilon = 0$ . We note that *by considering a vanishingly small (yet non-zero) temperature, it is possible to determine that the origin is not included within the closed contour, hence the transmission phase lapses by  $-\pi$  (rather than by  $+\pi$ ).*

For  $0 < T \ll \Delta, \Gamma$ , the evolution of the phase  $\theta_+$  for  $\epsilon \approx 0$  is well approximated by (see Appendix C)

$$\theta_+(\epsilon) \simeq \text{ArcTan}[\epsilon/\lambda] - \frac{\pi}{2}. \quad (12)$$

The width of the phase lapse is therefore given by a non-trivial combination of  $T$ ,  $\Gamma$  and  $\Delta$ :

$$\lambda \simeq (8\pi^2/3) \Gamma T^2 / \Delta^2. \quad (13)$$

We note that this contrasts with the width of the conductance peaks<sup>8</sup>,  $\lambda_{\text{peak}} \sim \max[\Gamma, T]$ . Therefore, the quadratic dependence of  $\lambda$  on the  $T$  leads at  $T, \Gamma \ll \Delta$  to the inequality

$$\lambda \ll \lambda_{\text{peak}} \text{ for } T, \Gamma \ll \Delta.$$

The smallness of  $\lambda$  is in qualitative agreement with experimental observations<sup>5</sup>.

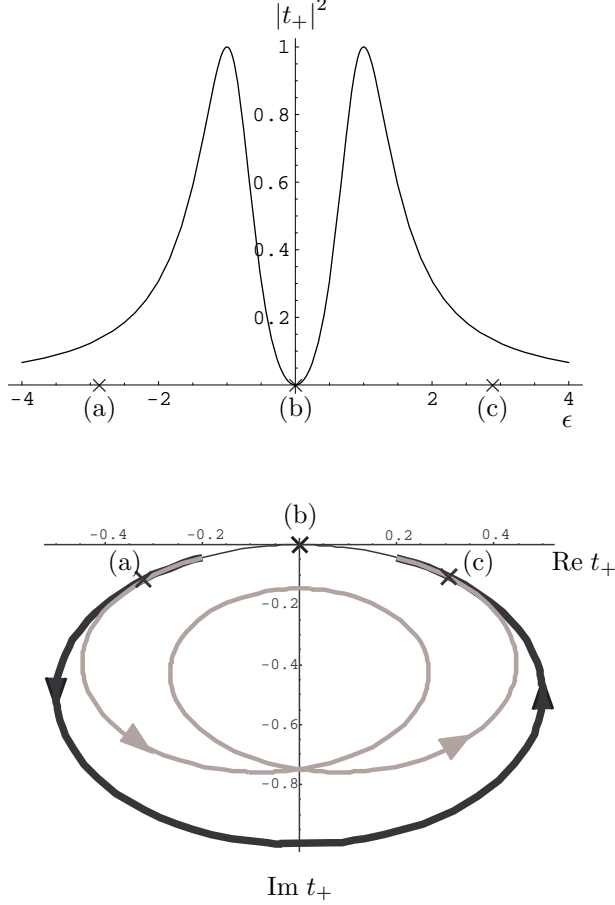


FIG. 4. Plot of  $|t_+(\epsilon)|^2$  vs.  $\epsilon$  for  $\epsilon_1 - \epsilon_2 = 2$  and  $\Gamma = 0.5$  (upper plot) and of  $t_+(\epsilon)$  in the complex plane (lower plot). At zero temperature the transmission amplitude evolves along a circle in the lower part of the complex plane ( $\text{Im}[t] \leq 0$ ). As  $\epsilon$  is increased,  $t_+(\epsilon)$  evolves from point (a) traversing the origin at  $\epsilon = 0$  [point (b)] and winds around the circle again up to point (c). The black thick line in the lower plot denotes that portion of the circle that is visited twice by  $t_+(\epsilon)$  as  $\epsilon$  varies from  $-4$  to  $4$ . Upon temperature averaging  $t_+(\epsilon)$  evolves along a contour enclosed in the zero temperature circle (grey line in the lower plot at  $T = 0.2$ ). As a result, the finite temperature curve does not contain the origin, and the phase lapse of Fig. 3 is smeared. It is then easily concluded that as  $T \rightarrow 0$  the transmission phase lapses by  $-\pi$ .

As seen from Fig. 2, the presence of a zero of the transmission amplitude implies that  $G(\epsilon)$  has a peak-valley-peak structure for *all* values of  $\Gamma$ . The width (but not

the depth) of the conductance valley shrinks as  $\Gamma$  is increased, and the value of the transmission probability at the peaks is always equal to 1.

## B. Differential Capacitance $C$ for $s = +1$

The features seen in the conductance are now contrasted with the behavior of the spectral density,  $A_+$  (at the Fermi energy) as a function of  $\epsilon$ , depicted in Fig. 5. Unlike the destructive interference that leads to the vanishing of the conductance at  $\epsilon = 0$ , the two peaks in the spectral density tend to *merge* into a single peak as  $\Gamma$  increases.

Formally the difference between these two quantities is seen in Eq. (A3) for the transmission and Eq. (A4) for the spectral density. While the former depends on all the elements of the Green function matrix, including the off-diagonal ones, the latter contains information on its trace only. Physically, the conductance depends directly on the size and signs of the couplings to the leads, as it describes the transfer of an electron from the left lead to the right one through both levels of the QD. The spectral density, on the other hand, depends on the couplings to the leads only through the modification of the position and width of the bare levels.

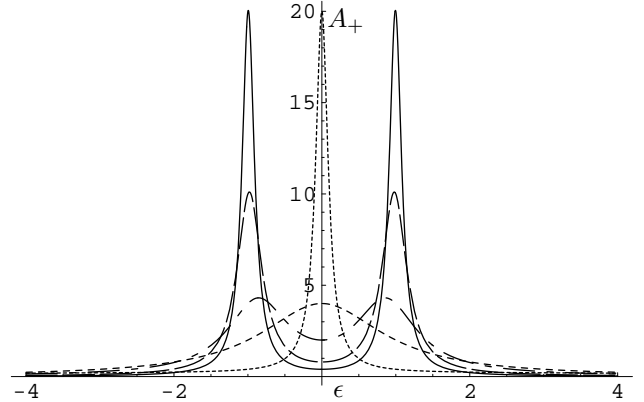


FIG. 5. The spectral density  $A_+$  [given by Eq. (10) and related to the differential capacitance via Eq. (16)], vs.  $\epsilon$  for  $s = +1$ . Here  $\epsilon_1 - \epsilon_2 = 2$  and  $\Gamma = 0.1$  (full),  $0.2$  (dashed),  $0.5$  (dash-dotted),  $1$  (dotted), and  $5$  (small dots). Note that unlike the conductance  $|t_+|^2$  depicted in Fig. 2, here there is a peak emerging at  $\epsilon = 0$  for large values of  $\Gamma$ .

To gain some insight into the behavior of the spectral density, it is useful to rewrite it as the sum of two Lorentzians

$$A_+(\omega) = -2 \text{Im} \left[ \frac{1}{\omega - \omega_e} + \frac{1}{\omega - \omega_o} \right], \quad (14)$$

where the poles are given by

$$\omega_{e(o)} = -\epsilon - i\Gamma \pm \sqrt{(\Delta/2)^2 - \Gamma^2}. \quad (15)$$

The expression for  $A_+(\omega)$  shows that for  $\Gamma \ll \Delta/2$  the two Lorentzians are centered at the positions of the original levels ( $\epsilon_{1,2}$ ) and have each a width  $\Gamma$ . As  $\Gamma$  exceeds  $\Delta/2$  the picture is drastically revised — in this limit the two peaks of the spectral density *merge* to form two peaks centered at  $-\epsilon$  with different widths  $\Gamma_{e(o)} = \Gamma \pm \sqrt{\Gamma^2 - (\Delta/2)^2}$ . Indeed, while one of these two peaks of  $A_+$  broadens as  $\Gamma$  is increased, the second one becomes increasingly sharper<sup>23</sup> (cf. Fig. 5). This behavior is directly reflected in the differential capacitance (as a function of  $V_g$ ). At zero temperature, the differential capacitance [Eq.(5)] of our toy model is given by

$$C(V_g) = e \frac{A(\omega = 0)}{2\pi}. \quad (16)$$

The fact that the transmission zero and the spectral *merging* occur concomitantly can be understood through a simple change of variables. Let us perform a canonical transformation to even and odd combinations of the dot's operators

$$d_e = \frac{d_1 + d_2}{\sqrt{2}}, \quad d_o = \frac{d_1 - d_2}{\sqrt{2}}. \quad (17)$$

Substituting in the Hamiltonian, Eq.(6), we obtain

$$H = \sum \epsilon_{k,i} c_{k,i}^\dagger c_{k,i} - \epsilon(d_o^\dagger d_o + d_e^\dagger d_e) + \frac{\Delta}{2}(d_e^\dagger d_o + h.c.) + \sum_k V \left[ (c_{k,L}^\dagger + c_{k,R}^\dagger) d_e + h.c. \right]. \quad (18)$$

In this representation, only one combination (even) is directly coupled to the leads. However, since both the even and odd modes are not eigenstates of the dot's Hamiltonian they are coupled by a tunneling term, whose strength is  $\Delta/2$ .

Employing this transformation, we readily understand the behavior of the spectral density for  $\Gamma \gtrsim \Delta/2$ . Indeed, in this case the two concentric peaks of the spectral density  $A_+$  essentially correspond to the even (broad peak) and odd (narrow peak) combinations respectively. The reason why in this limit it is particularly useful to stick to the even-odd basis is that the escape time  $1/\Gamma$  from the even combination to the leads is shorter than the typical time for tunneling between the two modes  $2/\Delta$ . Since the even mode is directly coupled to the leads its width is larger than that of the odd mode.

## V. ANALYSIS OF THE CASE $s = -1$

As anticipated in the introduction, the behavior described above is not universal but depends crucially on the relative sign of the coupling constants,  $s$ . Indeed, the qualitative features for  $s = -1$  are different from the ones described above for  $s = +1$ . In this case the spectral density assumes the form [cf. Eq.(10)]

$$A_-(\omega) = \frac{2\Gamma}{(\omega + \epsilon - \Delta)^2 + \Gamma^2} + \frac{2\Gamma}{(\omega + \epsilon + \Delta)^2 + \Gamma^2}, \quad (19)$$

while the transmission amplitude is given by [cf. Eq.(9)]

$$t_-(\omega) = \Gamma \left[ \frac{1}{\omega + \epsilon - \Delta + i\Gamma} - \frac{1}{\omega + \epsilon + \Delta + i\Gamma} \right]. \quad (20)$$

### A. The conductance $G$ and transmission phase $\theta$ for $s = -1$

We first consider the transmission probability depicted in Fig. 6. The features of the case  $s = -1$  are markedly different from the previous  $s = +1$  case. First, the transmission probability  $|t_-|^2$  is always finite over the entire energy ( $\epsilon$ ) range, implying the absence of a phase lapse. Indeed, the phase evolves continuously from zero to  $2\pi$  as  $\epsilon$  is swept across the two resonances.

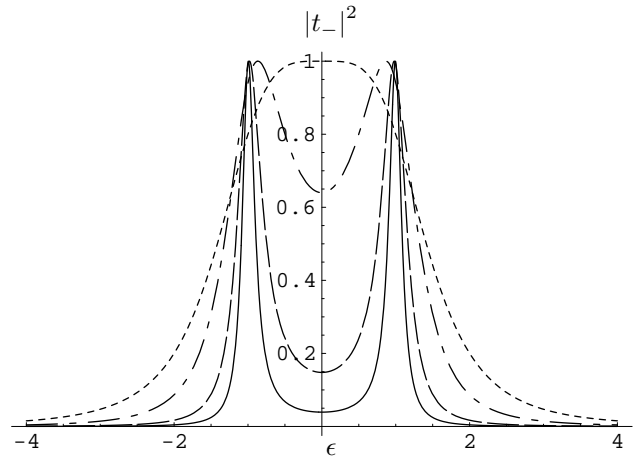


FIG. 6. The transmission probability  $|t_-|^2$  at the Fermi energy vs.  $\epsilon$  for  $s = -1$ . Here,  $\Delta = \epsilon_1 - \epsilon_2 = 2$  and  $\Gamma = 0.1$  (full), 0.2 (dashed), 0.5 (dash-dotted), 1 (dotted). Notice that in contrast to the zero at  $\epsilon = 0$  for  $s = +1$  (Fig. 2), here at large  $\Gamma$  the conductance is peaked at  $\epsilon = 0$ . In similarity to the spectral density  $A_+$  (Fig. 5), as  $\Gamma$  increases the conductance peaks approach each and subsequently merge<sup>24</sup>.

Secondly, the positions of the maxima of the transmission probability  $|t_-|^2$  shift as  $\Gamma$  is increased (contrary to the  $s = +1$  scenario, Fig. 3); they are given by  $\omega^\pm = -\epsilon \pm \sqrt{(\Delta/2)^2 - \Gamma^2}$  for  $\Gamma \lesssim \Delta/2$ . For  $\Gamma \gtrsim \Delta/2$  the two peaks merge<sup>24</sup> and are centered at  $-\epsilon$ . This behavior is reminiscent of the one observed in the spectral density in the  $s = +1$  case, cf. Fig. 5.

## VI. BRIEF SUMMARY AND POSSIBLE EXTENSIONS.

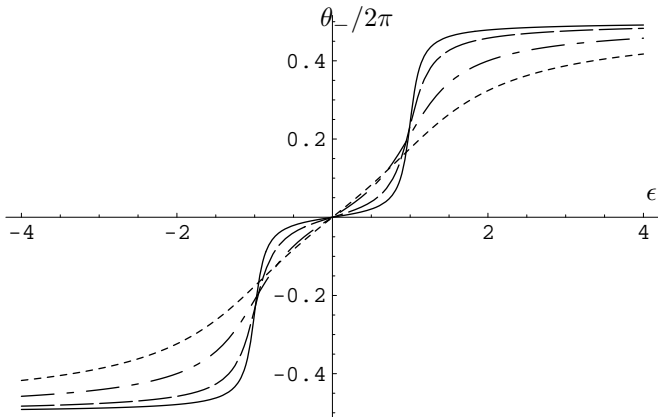


FIG. 7. The transmission phase  $\theta_-/2\pi$  at zero temperature vs.  $\epsilon$  for  $s = +1$ . Here,  $\Delta = \epsilon_1 - \epsilon_2 = 2$  and  $\Gamma = 0.1$  (full), 0.2 (dashed), 0.5 (dash-dotted), 1 (dotted). Notice that in contrast to Fig. 2 the phase evolves in the conductance valley continuously from zero to  $2\pi$ , hence no phase lapse.

It is quite interesting to note that for the present  $s = -1$  scenario the peaks in the spectral density do not shift (unlike the  $s = +1$  case). This is seen from Eq.(19) and Fig. 8.

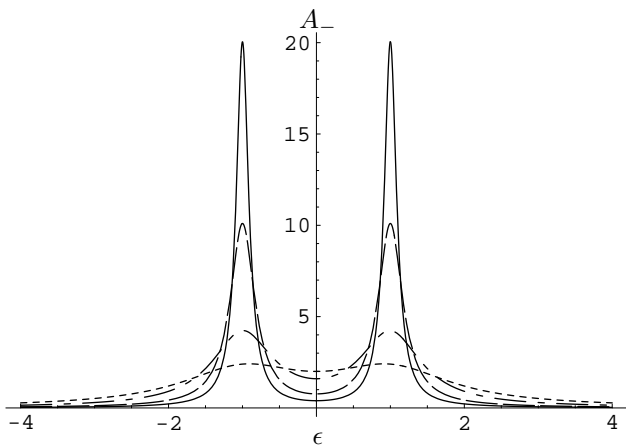


FIG. 8. The spectral density  $A_-$  at the Fermi energy vs.  $\epsilon$  for  $s = -1$ . Here  $\Delta = \epsilon_1 - \epsilon_2 = 2$  and  $\Gamma = 0.1$  (full), 0.2 (dashed), 0.5 (dash-dotted), 1 (dotted). Note that the peak positions do not depend on the strength of the coupling to the leads,  $\Gamma$ , similarly to the behavior of  $|t_+|^2$  depicted in Fig. 2.

A concise way to summarize the qualitative behavior of the cases  $s = \pm 1$  is by noting that  $|t_{\pm}|^2$  and  $A_{\pm}$  behave in a complementary manner as far as the peak position is concerned<sup>24</sup>. For both  $|t_+|^2$  and for  $A_-$  the peak positions are insensitive to the magnitude of  $\Gamma$ , while for both  $|t_-|^2$  and for  $A_+$  the peaks approach each other as  $\Gamma$  is increased and finally they merge. The reader may consult Table. I.

The preceding analysis was restricted to a toy model of a QD with two adjacent levels. The qualitative features described above would survive the extension of our model to  $N > 2$  levels. As  $\Gamma$  is increased towards  $\Delta$ , the crucial parameter determining the behavior of the conductance, the transmission phase and the spectral density is the relative sign of the coupling matrix elements associated with consecutive levels. As an example Fig. 9 and Fig. 10 depict the transmission probability  $|t|^2$  and the transmission phase  $\theta$  respectively for a set of 7 levels, the first four “in-phase” ( $s = +1$ ) while the next three levels being “out of-phase” ( $s = -1$ ). Similarly to the two-level model, we observe here zeroes of the transmission amplitude as well as phase lapses ( $s = +$ ). The peak structure for  $s = -1$  is blurred, indicating an incipient merger of the peaks (cf. Fig. 6).

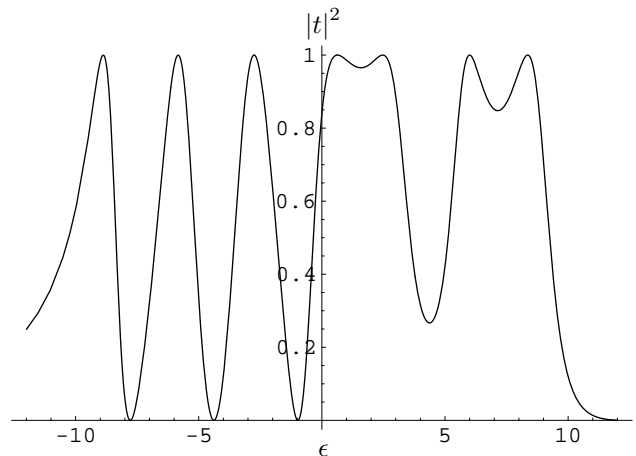


FIG. 9. The transmission probability  $|t|^2$  at the Fermi level vs.  $\epsilon$  for 7 levels, with level spacing  $\Delta = 3$ . All couplings to the leads have the same magnitude (for every level  $\Gamma = \Gamma_L + \Gamma_R = 1$ ). However, the first four levels are in phase, while the last three (peaks on the right) have a relative phase of  $\pi$  between each consecutive pair. Note that the “conductance valley” between, e.g., peaks 4 and 5 almost disappears. All the qualitative features described in the text for two levels are observed also here.

Once  $\Gamma, T \gg \Delta$  (for our noninteracting model) more than two levels will contribute to the transmission amplitude of electrons at a certain energy. In this case, for every value of the gate voltage, the details of the couplings to the leads (magnitude and phase) of a set of  $N \simeq \Gamma/\Delta$  levels around the Fermi level determine the behavior of the system.

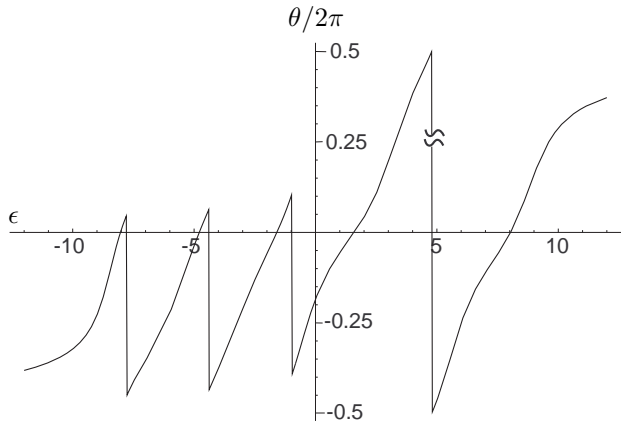


FIG. 10. The transmission phase  $\theta/2\pi$  vs.  $\epsilon$  for 7 levels, with level spacing  $\Delta = 3$ . All couplings to the leads have the same absolute value (for every level  $\Gamma = 1$ ) (cf. the caption of Fig. 9). Since the first four levels are “in phase” ( $s = +1$ ), a phase lapse of  $-\pi$  is observed in the valleys between peaks (1,2), (2,3), and (3,4). For the remaining levels, being “out of-phase”, the phase evolves continuously. The discontinuous jump seen at  $\epsilon \simeq 5$  is due to the fact that the phase is defined between 0 and  $2\pi$  and *does not* reflect any physical effect.

The issue of electron-electron interaction deserves careful consideration, beyond the scope of the present paper. A few remarks are nevertheless due. One can account for the interaction on the level of a capacitive term, incorporating the standard term

$$\hat{H}_{\text{int}} = U n_1 n_2 \quad (21)$$

( $n_i = d_i^\dagger d_i$ ) in the Hamiltonian [cf. Eq.(6)]. It is possible to treat this interaction term within a self-consistent

Hartree scheme. This approximation is justified<sup>25</sup> when  $\Gamma < \Delta$ . In this case the main relevant features of the model studied here, *i.e.*, the qualitative differences between the two cases  $s = +1$  and  $s = -1$  as well as the contrasting behavior of the conductance and the spectral density, remain unchanged. In particular, for  $s = +1$  the conductance valley contains a zero and therefore the phase exhibits a lapse in similitude to the noninteracting case. Within this scheme the main effect of including the interactions is the replacement of the bare levels  $\epsilon_1, \epsilon_2$  by the self consistent Hartree levels

$$\epsilon'_1 = \epsilon_1 + U \langle n_2 \rangle \quad ; \quad \epsilon'_2 = \epsilon_2 + U \langle n_1 \rangle. \quad (22)$$

It follows that the distance between consecutive conductance peaks is then  $\approx \Delta + U$ .

In conclusion, we have analyzed a simple noninteracting toy model describing a QD coupled to two leads and studied certain important observables such as the transmission amplitude through the QD (phase and magnitude), as well as the spectral density. We have shown that the transmission probability and the spectral density exhibit qualitatively different behavior as function of the plunger voltage. These differences become dramatically apparent when the coupling to the leads  $\Gamma$  exceeds  $\Delta$ .

A crucially important parameter in our discussion is the relative phase  $\varphi$  between two adjacent levels in the QD. The behavior of the various physical quantities depends strongly on whether this phase is  $\varphi = 0$  ( $s = +1$ ) or  $\varphi = \pi$  ( $s = -1$ ) (time reversal symmetry is assumed). The salient features observed in these two cases are summarized in Table I.

		$s = +1$	$s = -1$
$G$ :	Conductance	peaks do not shift	peaks merge at $\Gamma > \Delta/2$
$\theta$ :	Transmission phase	a sharp phase lapse of width $\propto \Gamma(T/\Delta)^2$	no phase lapse
$C$ :	Differential capacitance	peaks merge at $\Gamma > \Delta/2$	peaks do not shift

TABLE I. Notice the complementarity in the qualitative features of the differential capacitance and the conductance for  $s = +1$  and  $s = -1$ .

## VII. ACKNOWLEDGMENT

We would like to thank S. Levit, Y. Imry, M. Heiblum, M. Schechter, J. König and B. Kubala for helpful discussions. Y.G. and A.S. acknowledge the hospitality of ITP Santa Barbara where part of this work was performed. This work has been supported by the Israel Science Foundation of the Israel Academy grants, by the German-Israel DIP grants, by the U.S.-Israel BSF, and by the German-Israel GIF.

## APPENDIX A: DERIVATION OF THE TRANSMISSION AMPLITUDE AND SPECTRAL DENSITY

In this appendix we sketch the derivation of the transmission amplitude and the spectral density, Eqs.(9) and (10). All physical quantities discussed here can be expressed in terms of the QD Green’s functions  $\mathbf{G}_{i,j}(t) \equiv -i\theta(t)\langle d_i(t), d_j^\dagger(0) \rangle$ . This Green’s function matrix is given by

$$\mathbf{G}(\omega) = (\omega - \mathbf{H})^{-1}, \quad (A1)$$



where

$$\mathbf{H} = \begin{pmatrix} \epsilon_1 - i\Gamma & -i\Gamma e^{-i\varphi/2} \cos(\varphi/2) \\ -i\Gamma e^{i\varphi/2} \cos(\varphi/2) & \epsilon_2 - i\Gamma \end{pmatrix}, \quad (\text{A2})$$

is the effective Hamiltonian of the two level system, following the integration of the leads states. The width  $\Gamma$  is given by  $2\pi\rho V^2$ , where  $\rho$  is the DOS of the leads.

It is possible to write the transmission amplitude from left to right in terms of the matrix  $\mathbf{G}$

$$t(\omega) = 2\pi\rho \sum_{i,j=1,2} V_{L,i}^* [\mathbf{G}(\omega)]_{i,j} V_{R,j}. \quad (\text{A3})$$

Thus, the evaluation of the transmission amplitude requires knowledge of the diagonal and off-diagonal components of the matrix  $\mathbf{G}$ . On the other hand, the density of states in the QD involves only the diagonal components of  $\mathbf{G}$  and is given by

$$A(\omega) = -2\text{Im}[\text{tr}[\mathbf{G}(\omega)]] . \quad (\text{A4})$$

The calculation of  $\mathbf{G}(\omega)$  is straightforward and yields

$$\mathbf{G} = \frac{1}{D(\omega)} \begin{pmatrix} \omega + \epsilon + \Delta/2 + i\Gamma & -i\Gamma e^{-i\varphi/2} \cos(\varphi/2) \\ -i\Gamma e^{i\varphi/2} \cos(\varphi/2) & \omega + \epsilon - \Delta/2 + i\Gamma \end{pmatrix}, \quad (\text{A5})$$

where the denominator is  $D(\omega) = (\omega + \epsilon)^2 - (\Delta/2)^2 + 2i\Gamma(\omega + \epsilon) - \Gamma^2 \sin^2(\varphi/2)$ .

## APPENDIX B: INTERFERENCE AND OFF-DIAGONAL GREEN'S FUNCTIONS

In this appendix we show, by means of a perturbative expansion in  $\Gamma$ , that the contribution of the off-diagonal Green's functions to the transmission amplitude is crucial in obtaining a zero in  $t_+$  and therefore an abrupt phase lapse at  $T = 0$ .

Using Eq. (A3) as well as the expression for the Green's function matrix  $\mathbf{G}$ , Eq. (A5), one can write the transmission amplitude  $t_+$  as

$$t_+(\omega) = t_{\text{diag}}(\omega) + t_{\text{off}}(\omega), \quad (\text{B1})$$

$$t_{\text{diag}}(\omega) \equiv \Gamma \mathbf{G}_{1,1}(\omega) + \Gamma \mathbf{G}_{2,2}(\omega), \quad (\text{B2})$$

$$t_{\text{off}}(\omega) \equiv \Gamma \mathbf{G}_{1,2}(\omega) + \Gamma \mathbf{G}_{2,1}(\omega), \quad (\text{B3})$$

where  $t_{\text{diag(off)}}$  consists of the diagonal/(off-diagonal) contributions to  $t_+$ .

Let us now expand the two contributions to  $t_+$  up to second order in  $\Gamma$ . Setting  $\omega = 0$  one obtains

$$t_{\text{diag}}(0) \simeq -\frac{8\epsilon}{\Delta^2 - 4\epsilon^2} \Gamma - i \frac{8(\Delta^2 + 4\epsilon^2)}{(\Delta^2 - 4\epsilon^2)^2} \Gamma^2, \quad (\text{B4})$$

$$t_{\text{off}}(0) \simeq i \frac{8}{\Delta^2 - 4\epsilon^2} \Gamma^2. \quad (\text{B5})$$

The expansion of  $t_{\text{diag}}$  begins with the linear order in  $\Gamma$ , describing processes where an electron hops from the leads to the dot and out. This term is real and vanishes for  $\epsilon = 0$ . The imaginary part of  $t_{\text{diag}}$  is determined by the  $O(\Gamma^2)$  term in the perturbative expansion, describing events where an electron hops twice from the lead to the *same* level before being transferred through the dot. This term is of the same order in  $\Gamma$  as the leading term in the expansion of  $t_{\text{off}}$ , the latter describing events where an electron hops twice from the lead to *different* levels before being transferred through the dot (e.g., left lead  $\rightarrow$  level 1  $\rightarrow$  left lead  $\rightarrow$  level 2  $\rightarrow$  right lead). It turns out that the term  $O(\Gamma^2)$  in the perturbative expansion of  $t_{\text{off}}$  is purely imaginary and cancels exactly against the  $O(\Gamma^2)$  term of  $t_{\text{diag}}$  at  $\epsilon = 0$ . More generally, once the contribution of the off-diagonal Green's functions is included, the cancellations leading to an exact zero of the transmission amplitude appear order by order in the perturbative expansion in the dot-lead coupling.

## APPENDIX C: EVALUATION OF THE WIDTH OF THE PHASE LAPSE AT FINITE TEMPERATURES

In this appendix we derive the expression for the width of the phase lapse Eq. (13). The phase observed in an AB interference experiment,  $\theta$ , is defined in Eq.(3). Focusing on the case  $s = +1$ , the transmission amplitude Eq.(9) can be expressed as

$$t_+(\omega) = \frac{2\Gamma(\omega_o + \epsilon)}{(\omega_o - \omega_e)} \frac{1}{\omega - \omega_o} - \frac{2\Gamma(\omega_e + \epsilon)}{(\omega_o - \omega_e)} \frac{1}{\omega - \omega_e}, \quad (\text{C1})$$

where the poles  $\omega_{e,o}$  are given in Eq. (15). The *temperature averaged transmission amplitude* is therefore given by

$$\begin{aligned} t_+(T) &= - \int d\omega f'(\omega) t(\omega) \\ &= \frac{2\Gamma(\omega_o + \epsilon)}{(\omega_o - \omega_e)} \left[ \frac{1}{2\pi i T} \Psi' \left[ \frac{1}{2} + \frac{\omega_o}{2\pi i T} \right] \right] \\ &\quad - \frac{2\Gamma(\omega_e + \epsilon)}{(\omega_o - \omega_e)} \left[ \frac{1}{2\pi i T} \Psi' \left[ \frac{1}{2} + \frac{\omega_e}{2\pi i T} \right] \right], \quad (\text{C2}) \end{aligned}$$

where  $\Psi'$  is the trigamma function. In order to obtain the low temperature behavior of the transmission phase close to the phase lapse, one has to expand Eq.(C2) up to second order in  $\epsilon$  and  $T$  obtaining

$$\begin{aligned} t_+(T) &= -\frac{8\Gamma}{\Delta^2} \epsilon - i \frac{64\Gamma^2(\pi^2 T^2 + 3\epsilon^2)}{3\Delta^4} \\ &\simeq -\frac{8\Gamma}{\Delta^2} \epsilon - i \frac{64\Gamma^2 \pi^2}{3\Delta^4} T^2, \quad (\text{C3}) \end{aligned}$$

the last equality being valid for  $|\epsilon| \ll T$ . The width of the phase lapse,  $\lambda$ , in Eq. (13) follows. It is obtained straightforwardly from the expression for the temperature averaged transmission phase

$$\begin{aligned}\theta(T) &= \text{ArcTan} \left( -\frac{\text{Re}[t]}{\text{Im}[t]} \right) - \frac{\pi}{2} \\ &= \text{ArcTan} \left( -\frac{\epsilon}{\lambda} \right) - \frac{\pi}{2}.\end{aligned}\quad (\text{C4})$$

---

\* Incumbent of the Louis and Ida Rich career Development Chair.

<sup>1</sup> K. A. Matveev, Phys. Rev. B **51**, 1743 (1995).

<sup>2</sup> Yu. V. Nazarov, Phys. Rev. Lett. **82**, 1245 (1999).

<sup>3</sup> A. Kamenev, Phys. Rev. Lett. **85**, 4160-4163 (2000).

<sup>4</sup> I. L. Aleiner, P. W. Brouwer, I. L. Glazman, Phys. Rep. **358**, 309 (2002).

<sup>5</sup> A. Yacobi, M. Heiblum, D. Mahalu, and H. Shtrikman, Phys. Rev. Lett. **74**, 4047 (1995); R. Schuster, E. Bucks, M. Heiblum, D. Mahalu, V. Umansky, and H. Shtrikman, Nature (London) **385**, 417 (1997); Y. Ji, M. Heiblum, D. Sprinzak, D. Mahalu, H. Shtrikman, Science **290**, 779 (2000).

<sup>6</sup> R. Baltin and Y. Gefen, Phys. Rev. B **61**, 10247 (2000); R. Baltin, Y. Gefen, Phys. Rev. Lett. **83**, 5094 (1999); R. Baltin, Y. Gefen, G. Hackenbroich, H. A. Weidenmuller, European Physical Journal B **10**, 119 (1999).

<sup>7</sup> Y. Oreg and Y. Gefen, Phys. Rev. B **55**, 13726 (1997).

<sup>8</sup> L. P. Kouwenhoven, C. M. Marcus, P. L. McEuen, S. Tarucha, R. M. Westervelt, and N. S. Wingreen, in *Mesoscopic Electron Transport*, edited by L. L. Sohn, L. P. Kouwenhoven, and G. Schon (Kluwer, Dordrecht, 1997).

<sup>9</sup> Y. Meir and N. S. Wingreen, Phys. Rev. Lett. **68**, 2512 (1992).

<sup>10</sup> U. Gerland, J. von Delft, T. A. Costi, and Y. Oreg, Phys. Rev. Lett. **84**, 3710 (2000).

<sup>11</sup> J. König and Y. Gefen, Phys. Rev. Lett. **86**, 3855 (2001); J. König and Y. Gefen, Phys. Rev. B **65**045316-1 (2002).

<sup>12</sup> See, *e.g.*, A. Kaminski and L. I. Glazman, Phys. Rev. B **61**, 15927 (2000).

<sup>13</sup> O. Entin-Wohlman, A. Aharony, Y. Imry, Y. Levinson, cond-mat/0109328; O. Entin-Wohlman, A. Aharony, Y. Imry, Y. Levinson, A. Schiller, cond-mat/0108064.

<sup>14</sup> D. Feldman and Y. Gefen, unpublished.

<sup>15</sup> R. Berkovits, Y. Gefen, O. Entin-Wohlman, Philos. Mag. B **77**, 1123 (1998).

<sup>16</sup> G. Hackenbroich, W. D. Heiss, H. A. Weidenmuller, Philos. Mag. B **77**, 1255 (1998).

<sup>17</sup> H.-W. Lee, Phys. Rev. Lett. **82**, 2358 (1999); A. Levy Yeyati and M. Buttiker, Phys. Rev. B **62**, 7307 (2000);

P. G. Silvestrov and Y. Imry, Phys. Rev. Lett. **85**, 2565 (2000).

<sup>18</sup> D. Berman, N. B. Zhitenev, R. C. Ashoori, and M. Shayegan, Phys. Rev. Lett. **82**, 161 (1999).

<sup>19</sup> D. Sprinzak, Y. Ji, M. Heiblum, D. Mahalu, and H. Shtrikman, cond-mat/0109402.

<sup>20</sup> J. König, Y. Gefen, and G. Schon, Phys. Rev. Lett. **81**, 4468 (1998).

<sup>21</sup> Indeed, starting with a different phase for each coupling ( $V_{\alpha,j} = V \exp[i\varphi_{\alpha,j}]$ ), and applying the change of variables,  $\tilde{c}_{k,\alpha} = \exp[-i\varphi_{\alpha,1}] c_{k,\alpha}$ ,  $\tilde{d}_2 = \exp[i(\varphi_{L,2} - \varphi_{L,1})] d_2$ , and  $\tilde{d}_1 = d_1$ , one obtains an Hamiltonian of the form of Eq. 6 with hybridization couplings given by  $V_{L,1} = V_{R,1} = V_{L,2} = V$  and  $V_{R,2} = e^{i\varphi} V$ , where  $\varphi = (\varphi_{R,1} - \varphi_{R,2} - \varphi_{L,2} + \varphi_{L,1})$ .

<sup>22</sup> Allowing the four couplings to have different magnitudes leads to two main effects. If  $V_{L,1} = V_{L,2} \neq V_{R,1} = V_{R,2}$  (left/right asymmetry) the conductance is suppressed as a whole, but all the features described in the text (*e.g.*, zero of the conductance, the appearance of a phase lapse and the merging of the spectral density peaks for  $s = +1$ ) are still present. The other possible asymmetry,  $V_{L,1} = V_{R,1} \neq V_{R,2} = V_{L,2}$  (level asymmetry), spoils the symmetry of the conductance curve with respect to the point  $\epsilon = 0$ . The qualitative features discussed here remain intact, including the zero of the conductance (which is now shifted with respect to the  $\epsilon = 0$  point).

<sup>23</sup> A. Silva and S. Levit, unpublished; similar phenomena of spectral merging are observed in other context, see *e.g.* A. Abragam, *The Principles of Nuclear Magnetism*, Ch. 10, Oxford University Press (London), (1961).

<sup>24</sup> We note that though for  $\Gamma > \Delta/2$  both  $|t_-|^2$  and  $A_+$  have a single peak at  $\epsilon = 0$ , in one case the peak height diminishes as  $\Gamma$  is further increased ( $|t_-|^2$ ) while in the other case the central peak becomes more and more pronounced ( $A_+$ ).

<sup>25</sup> Note that for  $s = -1$  and in the presence of local Coulomb interaction it is possible, by means of change-of-variables  $c_{k,\uparrow} = (c_{k,L} + c_{k,R})/\sqrt{2}$ ,  $c_{k,\downarrow} = (c_{k,L} - c_{k,R})/\sqrt{2}$ , to map our model onto a pseudo-spin Anderson model<sup>26</sup>. Here, the indices  $\uparrow, \downarrow$  are the pseudo-spin states. In this language, the level spacing  $\Delta$  represents Zeeman splitting. It is known that this model could give rise to the Kondo effect, provided  $\Delta < T_K$  ( $T_K \ll \Gamma$ ), where  $T_K$  is the Kondo temperature. It follows that in this regime of the model the Hartree approximation is inappropriate since it erroneously breaks the SU(2) symmetry. For  $\Delta > \Gamma$  (hence  $\Delta \gg T_K$ ) the pseudo-spin SU(2) symmetry is broken, the Kondo effect is suppressed, and employment of the Hartree approximation is valid.

<sup>26</sup> W. Hofstetter, J. König, and H. Schoeller, Phys. Rev. Lett. **87**, 156803 (2001); D. Boese, W. Hofstetter, and H. Schoeller, cond-mat/0201461.